



Article

Genome-Wide Identification of CsATGs in Tea Plant and the Involvement of CsATG8e in Nitrogen Utilization

Wei Huang^{1,2}, Dan-Ni Ma^{1,2}, Hong-Ling Liu^{1,2}, Jie Luo^{1,2,3}, Pu Wang^{1,2}, Ming-Le Wang^{1,2}, Fei Guo^{1,2}, Yu Wang^{1,2}, Hua Zhao^{1,2,*}  and De-Jiang Ni^{1,2}

¹ Key Laboratory of Horticultural Plant Biology of Ministry of Education, Huazhong Agricultural University, Wuhan 430070, China; huangwtea@webmail.hzau.edu.cn (W.H.); madanni@webmail.hzau.edu.cn (D.-N.M.); liuhongling@webmail.hzau.edu.cn (H.-L.L.); luojie@mail.hzau.edu.cn (J.L.); pwang@mail.hzau.edu.cn (P.W.); wangmingle@mail.hzau.edu.cn (M.-L.W.); guofei@mail.hzau.edu.cn (F.G.); catea37@mail.hzau.edu.cn (Y.W.); nidj@mail.hzau.edu.cn (D.-J.N.)

² College of Horticulture and Forestry Sciences, Huazhong Agricultural University, Wuhan 430070, China

³ Hubei Engineering Technology Research Center for Forestry Information, Huazhong Agricultural University, Wuhan 430070, China

* Correspondence: zhaohua@mail.hzau.edu.cn

Received: 11 August 2020; Accepted: 22 September 2020; Published: 24 September 2020



Abstract: Nitrogen (N) is a macroelement with an indispensable role in the growth and development of plants, and tea plant (*Camellia sinensis*) is an evergreen perennial woody species with young shoots for harvest. During senescence or upon N stress, autophagy has been shown to be induced in leaves, involving a variety of autophagy-related genes (ATGs), which have not been characterized in tea plant yet. In this study, a genome-wide survey in tea plant genome identified a total of 80 *Camellia Sinensis* autophagy-related genes, CsATGs. The expression of CsATGs in the tea plant showed an obvious increase from S1 (stage 1) to S4 (stage 4), especially for CsATG8e. The expression levels of AtATGs (*Arabidopsis thaliana*) and genes involved in N transport and assimilation were greatly improved in CsATG8e-overexpressed *Arabidopsis*. Compared with wild type, the overexpression plants showed earlier bolting, an increase in amino N content, as well as a decrease in biomass and the levels of N, phosphorus and potassium. However, the N level was found significantly higher in APER (aerial part excluding rosette) in the overexpression plants relative to wild type. All these results demonstrated a convincing function of CsATG8e in N remobilization and plant development, indicating CsATG8e as a potential gene for modifying plant nutrient utilization.

Keywords: autophagy-related genes; *Camellia sinensis*; CsATG8e; nitrogen

1. Introduction

Tea plant (*Camellia sinensis*, (L.) O. Kuntze), a widely cultivated horticultural crop, is a perennial evergreen woody plant [1]. Nitrogen (N) is one of the most important contributors for tea plant growth and leaf quality due to the harvest of leaves several times a year [2]. A large amount of N is required for rounds of buds sprout for a whole year to achieve considerable yield and top quality, which is especially true in spring. Additionally, pruning is usually performed by the end of plucking season, leading to the removal of a significant amount of N. All this suggests a huge demand of N in tea plantation. To solve this demand, excessive N is usually fertilized to maintain the vigorous growth and tea yield, resulting in many environmental problems [3,4]. Meanwhile, plants also take N through leaves [5,6], but no such genes have been reported in tea plant yet. Apart from the uptake of N from soil as well as foliar, N remobilization within plants plays an important role in meeting the demand of young leaves. Under insufficient N conditions, N remobilization becomes a more important N source for growing shoots [7].

Autophagy (macro-autophagy) is a highly conserved cellular degradation process, with portions of cytosol and organelles broken down and the resulting macromolecules eventually recycled [8]. During this process, the unwanted macromolecular substances or damaged organelles are first sequestered into a double membrane structure called an autophagosome, followed by fusing the outer membrane of the autophagosome with the vacuolar membrane to release the cargos and inner membrane structures into the vacuole for degradation and recycling [9]. Under normal growth conditions, autophagy occurs at a low basal level to maintain cell homeostasis. However, in response to stresses of nutrient-limited conditions and senescence, autophagy will be stimulated to alleviate these stresses for plant survival [10,11]. In plants, autophagy has been demonstrated to associate with N remobilization during leaf senescence and grain filling [12,13]. Several confirmation studies have been performed on autophagy mutants of *Arabidopsis* and cereal crops. For example, in rice, Wada et al. [14] showed that the N remobilization in senescent leaves was suppressed in the mutant *Osatg7-1* (*Oryza sativa*, Os). In maize, the investigation of N partitioning in the mutant *Zmatg12* (*Zea mays*, Zm) showed an impaired N remobilization, leading to a significant decrease in seed yield [11]. In *Arabidopsis*, under both low and high nitrate conditions, supplying $^{15}\text{NO}_3^-$ during the vegetative stage led to a sharp decrease in ^{15}N remobilization in the mutants *atg5-1* and *atg9-2* relative to wild type in seeds at harvest [15].

Autophagy (ATG) genes, the main implementers and regulators of the autophagy process, were firstly characterized in yeast [16]. Since then, a number of ATG genes in single copy or subfamilies have been gradually identified in plants, such as *ATG1-13*, *16*, *18*, *101*, *VPS15* and *VPS34* [8,17,18]. According to the process of autophagy, these genes were classified into six functional complexes, with three of them as core autophagy genes in yeast, mammals and plants, including ATG9 recycling system, PI3K (Phosphoinositide 3-kinase) nucleation complex and two ubiquitin-like conjugation systems [18]. Genome-wide ATG genes have been systemically identified in many higher plants, such as 40 *AtATGs* in *Arabidopsis* [19] (*Arabidopsis*, At), 33 *OsATGs* in rice [14], 45 *ZmATGs* in maize [11] and 35 *VvATGs* in grapevine [20] (*Vitis vinifera*, Vv). However, no systemic reports are available about ATG genes in tea plant yet. In 2017, the first genome data for tea plant were released [21], followed by the successive release of several other genome data of *Camellia sinensis* for different cultivars [22,23], which provide useful information for understanding the ATG gene families in *Camellia sinensis*.

ATG8, a ubiquitin-like protein conjugated to phosphatidylethanolamine on the autophagic membrane, plays a central role in autophagy [24]. In plants, ATG8 is a family with multiple numbers, such as nine *AtATG8s* in *Arabidopsis* [25], six *VvATG8s* in grapevine [20] and five *OsATG8s* in rice [14]. Studies have indicated that ATG8 is beneficial to the plant performance in N utilization. For example, in apple, the expression of *MdATG8i* was induced in response to leaf senescence and N depletion, and the heterologous expression of *MdATG8i* (*Malus domestica*, Md) in *Arabidopsis* enhanced vegetative growth, leaf senescence and tolerance to N limitation [26]. Similarly, in rice, the expression of *OsATG8c* was enhanced during N starvation conditions, and the *35S-OsATG8c* rice plants showed an increase in yield as well as nitrogen uptake efficiency (NUpE) and nitrogen use efficiency (NUE) under both optimal and suboptimal N conditions [27]. Recently, Chen et al. [28] have shown that the overexpression of *AtATG8s* (*AtATG8a*, *AtATG8e*, *AtATG8f* and *AtATG8g*) with different promoters enhanced autophagosome number, promoted autophagy activity and increased the N remobilization efficiency under optimal N conditions without a negative effect on yield or biomass. Besides N, autophagy is also involved in recycling other nutrients, such as iron, zinc, manganese and sulfur [29–31]. Despite the characterization of the involvement of ATG8s in N remobilization and the participation of autophagy in recycling other nutrients in a number of plant species, little is known about them in tea plant.

In this study, a comprehensive investigation was performed about the *CsATG* families in the tea plant genome and a total of 80 *CsATGs* were identified. The gene structures, conserved domains and localizations on chromosomes were analyzed. Additionally, the phylogenetic trees were constructed along with their homologous genes from *Arabidopsis*, grapevine and sweet orange. Furthermore, we examined the expression patterns of *CsATG8s* in the leaves collected at four different stages from

three tea plant cultivars, and the importance of autophagy in tea plant was explored by analyzing the expression profiles of 16 *CsATGs* in response to various N conditions. Finally, *CsATG8e* was functionally characterized to identify its functional mechanisms in response to various N supplies by heterologous expression in *Arabidopsis*.

2. Results

2.1. Genome-Wide Identification of *CsATGs* in Tea Plant

A BLASTp (Protein Basic Local Alignment Search Tool) search was performed using ATG sequences from *Arabidopsis*, *Citrus sinensis* and *Vitis vinifera* as the queries against the tea plant genome database. After confirming the conserved domains of ATGs in the predicted sequences, a total of 80 putative *CsATGs* from 24 subfamilies were identified. Among them, the subfamilies vary greatly in the number of gene members (Supplementary Table S1), with the largest number in the *CsATG18* subfamily (18 members), followed by the *CsATG8* subfamily (12 members). Another twelve of the 24 subfamilies consist of more than one member, with 8 members in the *CsATG16* family, 5 members in the *CsATG1* family, 4 members in both *CsATG20* and *CsVPS35* families and the remaining ten subfamilies contain a single member, including *CsATG2*, *CsATG5*, *CsATG6*, *CsATG10*, *CsATG11*, *CsATG13*, *CsATG101*, *CsATI*, *CsNBR1* and *CsVPS34*. The members in some subfamilies were named based on the similarity to the other three species, while the other members were named randomly, as shown in Supplementary Table S1.

The physiological and biochemical parameters of all family members identified from tea plant are shown in Supplementary Table S1. The genomic sequence length of the 80 genes ranges from 375 bp (*CsATG1b*) to 39,472 bp (*CsATG11*) with open reading frame (ORF) length varying between 219 bp (*CsATG12b*) and 5994 bp (*CsATG2*). The protein size of the 80 proteins ranges from 72 aa (*CsATG12b*) to 1997 aa (*CsATG2*), with an average molecular weight (MW) of 8.2 to 218.7 kDa. The predicted theoretical isoelectric point (PI) ranges from 4.5 (*CsATI*) to 9.9 (*CsATG18a*), with 40 proteins under 7.0, 38 proteins above 7.0 and 2 at 7.0, indicating that the ATG proteins are widely distributed under alkaline, acidic and neutral conditions. Collectively, the 80 *CsATGs* vary greatly in the length of genome and ORF, protein size, MW and PI, even in a subfamily of *ATG8* or *ATG18*, implying their functional divergence.

2.2. Bioinformatic Characterization of the 80 *CsATGs*

2.2.1. Chromosomal Distribution of *CsATGs*

The chromosomal locations of *CsATGs* are shown in Figure 1a. Among the 80 *CsATGs*, 63 are widely distributed across the 15 chromosomes, and the other 17 genes are located on the 17 unassembled scaffolds (or assembled contigs), due to the incomplete physical map of *Camellia sinensis*. Chromosome 1 was predicted to contain the largest number of members (nine), followed by chromosome 2 (eight) and chromosome 4 (seven). On chromosomes 5, 9, 12, 13, 14 and 15, each contained two *ATG* members. As duplication usually contributes to the expansion of gene families, we investigated the duplication patterns of genes in one of the subfamilies containing more than one member. No tandem duplication gene was found, while a total of 31 genes were produced from the eight subfamilies of *CsATG1*, *CsATG3*, *CsATG7*, *CsATG8*, *CsATG16*, *CsATG18*, *CsVPS15* and *CsVPS35* by whole genome duplication (WGD), which constructed 25 pairs of collinear genes (Figure 1b, Supplementary Table S2). This suggests that WGD plays an important role in duplication of these gene subfamilies in tea plant. We also investigated the evolutionary processes in subfamily by the Ka/Ks (the ratio of nonsynonymous substitution to synonymous substitution) value but failed to obtain the value for one pair of genes (*CsATG8i* and *CsATG8h*) because they share the same coding sequence (CDS) despite their different localizations on chromosomes. Meanwhile, the Ka/Ks value is slightly higher than "1" (1.2279) for another pair of genes (*CsATG18q* and *CsATG18r*), but lower than "1" for the other 23 pairs of collinear genes. Purifying

selection usually works with $K_a/K_s < 1$; otherwise, positive selection occurs once the value is far higher than “1” [32]. Overall, purifying selection plays a primary role in the ATG subfamily members and positive selection is also necessary during the evolutionary history.

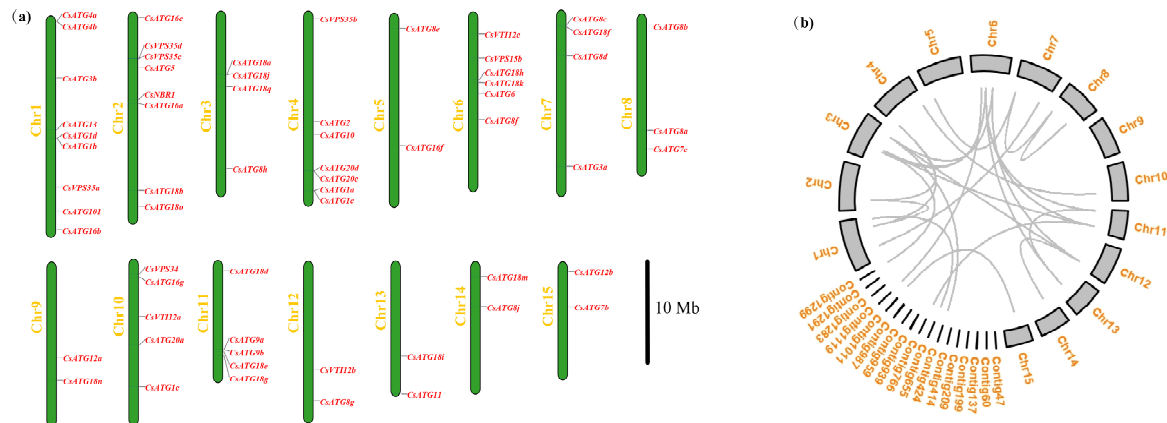


Figure 1. Chromosomal distribution and gene duplication of CsATG genes. (a) The distribution of 63 CsATG genes in 15 chromosomes. (b) The chromosomes and contigs containing the 80 CsATG genes, and the collinear pairs illustrated with one gray curve for one pair.

2.2.2. Phylogenetic Analysis

To explore the phylogenetic relationship among proteins in a subfamily, the neighbor-joining phylogenetic trees of the 24 subfamilies were constructed respectively based on the predicted amino acid sequences of each ATG subfamily in tea plant along with the ATG proteins from *Arabidopsis* and the two woody plants of grapevine (*Vitis vinifera*) and sweet orange (*Citrus sinensis*) (Figure 2). For the ATGs with a single member in a subfamily, the CsATGs were closely clustered with their homologues in a grapevine, excluding CsNBR1, which was more closely clustered with sweet orange than the other two species. As for the subfamilies with multiple members, some were clustered into one branch, such as CsATG3, CsATG4, CsATG14, CsATG20 and CsVPS15, and some were clustered into several branches, including CsATG1, CsATG8, CsATG9, CsATG12, CsATG16, CsATG18 and CsVPS35. Intriguingly, the four members in CsATG1 (CsATG1a, CsATG1c, CsATG1d and CsATG1e) were grouped more closely with the homologous genes in *Arabidopsis* than woody plants, indicating their potential functional similarity to *Arabidopsis*. These results suggested a closer relationship of tea plant with woody plants, especially grapevine, and also implied its potential functional differentiations within multiple subfamilies.

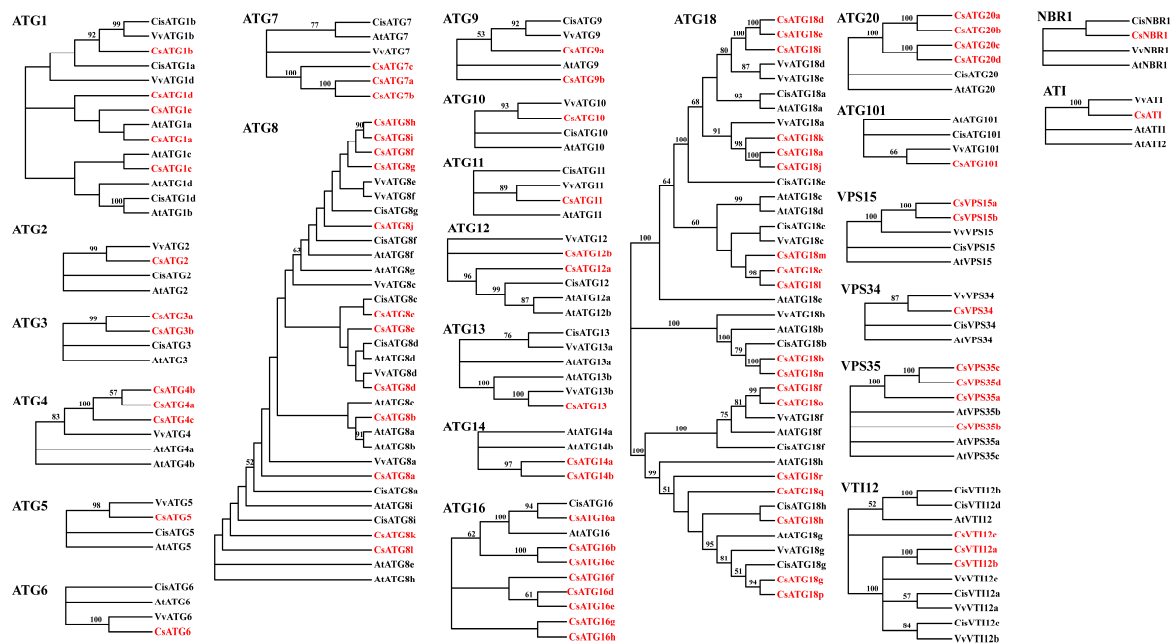


Figure 2. Phylogenetic analysis of *Camellia sinensis* and other plant ATG proteins. The neighbor-joining trees were constructed with 80 CsATGs of *Camellia sinensis* (Cs), 49 AtATGs of *Arabidopsis thaliana* (At), 37 CisATGs of *Citrus sinensis* (Cis) and 35 VvATGs of *Vitis vinifera* (Vv) using the MEGA-X software, with 1000 bootstrap replicates, and displayed without the tree root using the online tool iTOL (<https://itol.embl.de/>). The genes of tea plant are marked in red color. The bootstrap values higher than 50% are shown in the phylogenetic trees.

2.2.3. Gene Structures and Conserved Domains

The gene structures of all ATGs were presented and the domain compositions were analyzed by comparison with the corresponding proteins of *Arabidopsis* (Supplementary Table S3). As shown in Figure 3, among these 80 CsATGs, there was only one exon in the three genes of *CsATG16f*, *CsVTI12a* and *CsVTI12b*. However, for the other CsATGs, the number of exons ranged from two (*CsATG1b*, *CsATI* and *CsATG16g*) to 25 (*CsVPS35b*). The variations in exon number can show the diversity in a subfamily with multiple members. For instance, no variation was found in the exon number in the subfamily of *CsATG3* (9 exons), *CsATG7* (14 exons), *CsATG14* (12 exons), *CsATG20* (10 exons) and *CsVPS15* (11 exons). A limited variation was observed in the number of exons in the subfamilies of *CsVPS35* (22 and 25 exons) and *CsATG8* (5 and 6 exons). A great variation was found in the number of exons for some subfamilies, ranging from 2 to 11 in *CsATG1*, 3 to 11 in *CsATG18* and 1 to 16 in *CsATG1*. For the untranslated regions (UTRs), the longest one was found in *CsATG18c* at 5'-UTR, with both 5'-UTR and 3'-UTR observed in 33 genes, only 5'-UTR in 6 genes and just 3'-UTR in 11 genes. Additionally, we analyzed the conserved domains by comparing the 80 ATG proteins with the corresponding proteins in *Arabidopsis* (Supplementary Table S3). Except for *CsATI* without the domain of *AtATI* in *Arabidopsis*, the remaining 79 genes had 1 to 3 (5 for *CsNBR1*) domains, which can be found in *Arabidopsis* for the same subfamily, including ATG_C, Chorein_N, Autophagy_N, Peptidase_C54, E1_like_apg7, Ubl_ATG8, WD40, BCAS3, etc. However, some differences were observed between *Arabidopsis* and tea plant. For example, in *ATG1*, the domain PKc_like superfamily was found in the four subfamily members (*CsATG1a*, *CsATG1b*, *CsATG1d* and *CsATG1e*) in tea plant, but not in *Arabidopsis*. Meanwhile, for the *ATG11* subfamily, an APG17 superfamily domain was found in *Arabidopsis*, but not in tea plant. The CsATGs in a subfamily with the same domains might show functional similarity, in contrast to functional differentiation between subfamily members with different domains.

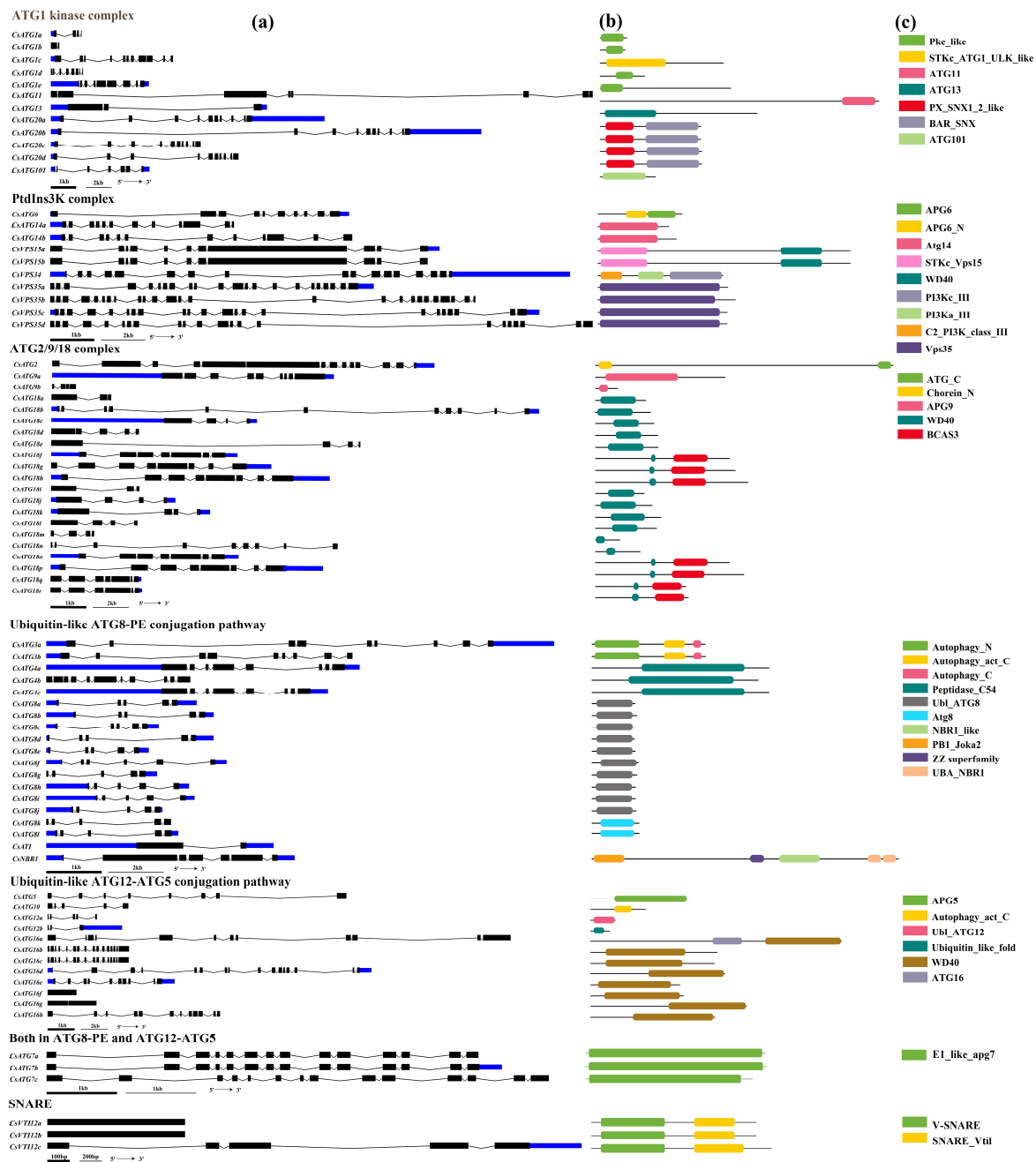


Figure 3. Gene structures and domains of *CsATG* genes in tea plant. (a) The exon-intron structures, with untranslated regions (UTRs) in blue rectangles, exons in black rectangles and introns in thin black lines. Domains of the corresponding genes on the left side (b,c). The 80 *CsATG* genes were presented according to their functions in autophagy.

2.3. Expression Profiles of *CsATGs* in *Camellia sinensis*

2.3.1. Expression Patterns for *CsATG8s* in Tea Cultivars

For evergreen perennial plants, the nutrient allocation within the plant is assumed to vary dynamically within tissues at different stages. To illustrate this assumption, we investigated the expressions of *CsATG8s* (ten out of twelve members, with the same amino acid sequences in *CsATG8h* and *CsATG8i*, *CsATG8k* and *CsATG8l* respectively, Supplementary Table S4 and Supplementary Figure S1b) in leaves at four different stages in the three green cultivars of *Fuding Dabai*, *Echa 10* and

Zhongcha 108. As shown in Figure 4a, all the tested genes showed the highest expression at S4 except for *CsATG8d* in *Fuding Dabai* and *CsATG8k* in *Echa 10*. Additionally, an upward tendency was observed from S1 to S4 in all the three cultivars in the expression of *CsATG8a*, *CsATG8e* and *CsATG8g*, especially *CsATG8e*, suggesting the potential role of *CsATG8e* in nutrient redistribution in tea plant.

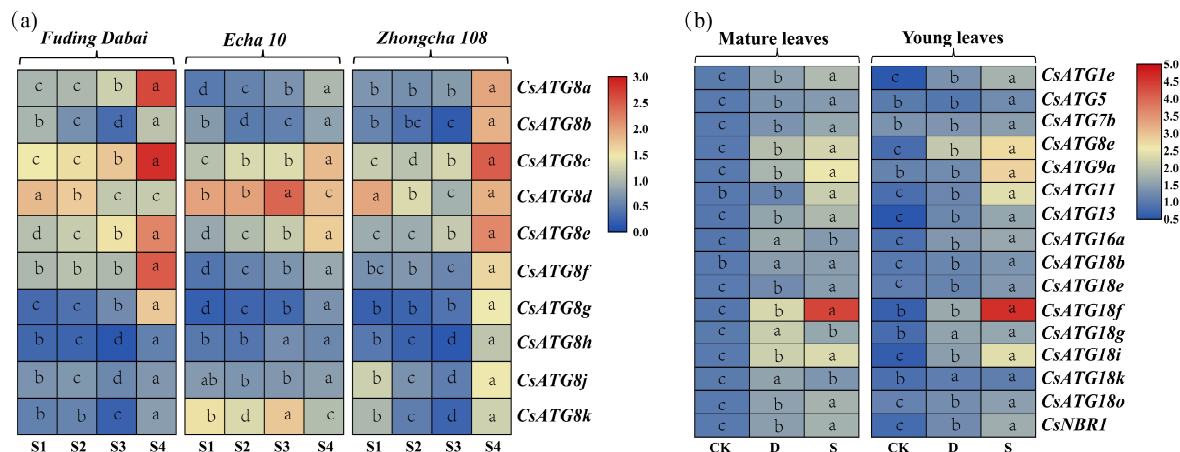


Figure 4. Expression patterns of *CsATG* genes in *Camellia sinensis*. (a) The expression of *CsATG8s* in the leaves at four different stages (S1, Stage 1; S2, Stage 2; S3, Stage 3; S4, Stage 4) in tea cultivars of *Fuding Dabai*, *Echa 10* and *Zhongcha 108*. (b) The expression of sixteen *CsATG* genes in *Zhongcha 108* under different N treatments. Y, young leaves; M, mature leaves; D, N-deficient, 0.125 mM NH_4NO_3 ; S, N-sufficient, 2.50 mM NH_4NO_3 ; CK, control. Different lowercase letters in rectangles indicate significant differences at $p < 0.05$ by analysis of variance (ANOVA) Duncan comparison.

2.3.2. Expression Patterns for *CsATGs* in Response to N

To explore the expression patterns of *CsATGs* in response to N, *Zhongcha 108* was selected and treated with two N levels: sufficient (5 mM N, 2.50 mM NH_4NO_3) and deficient (0.25 mM N, 0.125 mM NH_4NO_3), based on the expression patterns of *CsATG8s* in *Fuding Dabai*, *Echa 10* and *Zhongcha 108*. As the total number of identified *CsATGs* was up to 80, sixteen *CsATGs* were randomly chosen here from the members of relatively large subfamilies or key genes in autophagy process. qRT-PCR (quantitative reverse-transcription polymerase chain reaction) was used to investigate the expression patterns of the selected *CsATGs* in the young and the mature leaves under exposure to the two N conditions (5 and 0.25 mM). As shown in Figure 4b, a steady up-regulation was observed in both young and mature leaves in most of the sixteen *CsATGs* under N deficiency and sufficient conditions relative to their respective control, with the upregulation being more obvious under the sufficient N condition, especially for *CsATG18f* in both young and mature leaves. Additionally, the changes were more obvious in mature leaves than in young leaves when compared with their respective control. Among them, the transcript levels of *CsATG8e* showed the most obvious changes in both leaves under both sufficient and deficient N conditions. Overall, all the selected *CsATGs* were stimulated in response to N, with a higher variation in the response of *CsATG8e* to N changes in tea plant.

2.4. Cloning and Functional Characterization of *CsATG8e*

2.4.1. Cloning of *CsATG8e* and Comparison with *ATG8s* in *Camellia sinensis* and *Arabidopsis*

To investigate its function in tea plant, the 360 bp ORF of *CsATG8e* was cloned from *Fuding Dabai*. *CsATG8e* shared 4.28% to 89.08% identity with the *AtATG8* members in *Arabidopsis*, with the highest sequence similarity to *AtATG8c*, while the smallest similarity to *AtATG8e* (Supplementary Figure S1a). Meanwhile, *CsATG8e* shared 45.38% (*CsATG8l*) to 95.80% (*CsATG8c*) identity with the members of the *CsATG8* subfamily in *Camellia sinensis* (Supplementary Figure S1b). These results illustrated a higher similarity with homology proteins in tea plant than in *Arabidopsis*, and *CsATG8e* showed more sequence

similarity to *ATG8c* in both *Arabidopsis* and *Camellia sinensis*. Based on the amino acid sequences, ATG8 proteins can be divided into three groups: clade I (a), clade I (b) and clade II [33]. However, according to our phylogenetic analysis of CsATG8s (Figure 2), no clear classification was found for CsATG8s in tea plant. Thus, we investigated the amino acid sequences of CsATG8 proteins, and found a lack of an extra amino acid residue in CsATG8d and CsATG8f at the C-terminus after the glycine residue, similar to AtATG8h and AtATG8i, which belong to clade II. In our phylogenetic analysis, CsATG8e and AtATG8d (a member from clade I (a)) were classified into one group, implying CsATG8e belongs to clade I (a).

2.4.2. Transgenic Plants Promote Development but Decrease Biomass

To gain insight into how *CsATG8e* functions in response to N, the *CsATG8e*-overexpressed *Arabidopsis* plants were generated, and hydroponic growth conditions were established to figure out the progressive changes in response to three N regimes: low (0.25 mM N, 0.125 mM NH_4NO_3), moderate (1 mM N, 0.50 mM NH_4NO_3) and sufficient (5 mM N, 2.50 mM NH_4NO_3). After a 20-day culture under the sufficient N condition, an obvious difference was observed in the vegetative shoot between wild-type (WT) plants and overexpression (OE) plants (Figure 5a). Specifically, the inflorescences were visible in the OE plants while the WT plants were still in the vegetative growth stage, indicating the significant effect of *CsATG8e* on the development of overexpression plants.

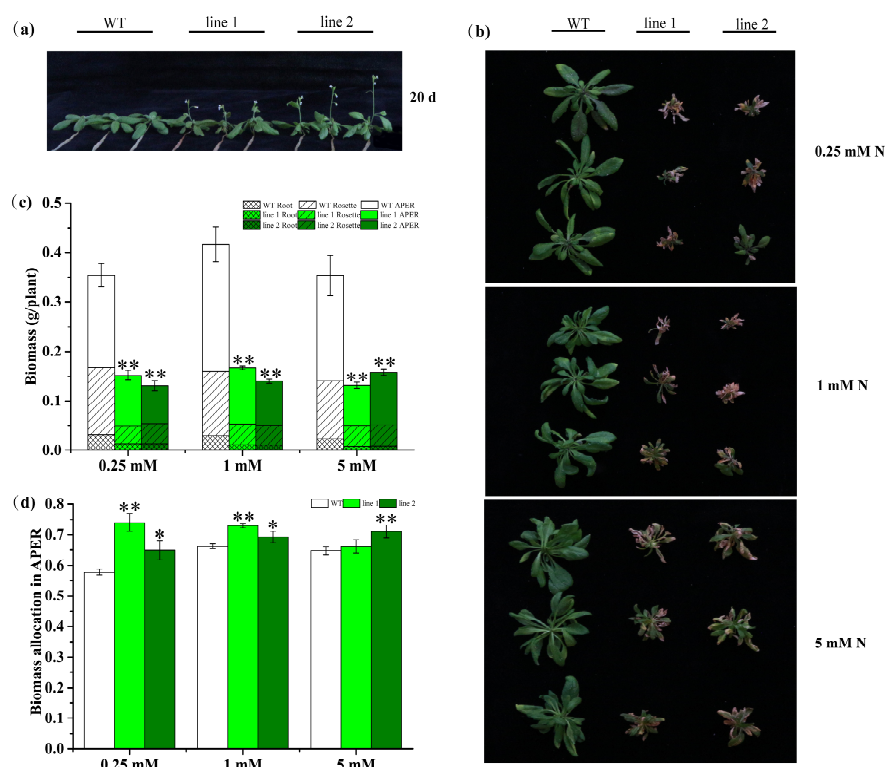


Figure 5. Comparison of growth performance between *CsATG8e*-overexpressed *Arabidopsis* (OE) and wild-type (WT) plants. (a) Growth of the WT and *CsATG8e* OE *Arabidopsis* after a 20-day culture at the sufficient N condition. (b) The rosette of OE and WT *Arabidopsis* after a 20-day culture under sufficient N, followed by another fourteen-day culture under different N levels. (c) The comparison of biomass in aerial part excluding rosette (APER), rosettes (Rosette) and roots (Root) between OE lines and WT. (d) The allocation of biomass in APER. 0.25 mM N, 0.125 mM NH_4NO_3 ; 1 mM N, 0.50 mM NH_4NO_3 ; 5 mM N, 2.50 mM NH_4NO_3 . Values are means \pm standard (SD) ($n \geq 6$). Asterisks indicate significant differences between WT and two OE lines (line 1, line 2). * $p < 0.05$; ** $p < 0.01$ (t -test).

After two weeks of growth under the three N regimes, compared with WT, the rosette of OE plants showed obvious purple and serious senescence, and a smaller size, regardless of the N supply level (Figure 5b). We examined the biomass of roots (Root), rosettes (Rosette) and aerial part excluding rosette (APER), and a decrease was observed in the biomass of Root, Rosette and APER in OE plants versus WT plants (Figure 5c). Considering that the buds or the tender leaves are usually harvested in tea plant, while in *Arabidopsis*, the APER came up after rosette formation, we investigated the biomass allocation in aerial part and defined biomass allocation in APER as $APER/(APER + Rosette)$ in this study. The biomass allocation in APER was found to be significantly higher than that of WT under all the three N regimes (Figure 5d). Collectively, the overexpression of *CsATG8e* in *Arabidopsis* led to earlier flowering and decreased biomass, regardless of N conditions.

2.4.3. Transgenic Plants Enhance N Use Capacity under Both Sufficient and Deficient N Conditions

To confirm whether autophagy differences exist between wild-type and transgenic plants, we investigated the expression patterns of 11 genes (*AtATG9*, *AtNBR1* and 9 genes in ubiquitin-like conjugation pathways) in the leaves after N treatment at 0.25 and 5 mM for one week (Figure 6a,d). A significantly ($p < 0.01$) upregulated expression was observed in OE lines under both N treatments, except for *AtATG8c* under the deficient N condition. We further examined the expression profiles of some genes related to N uptake, transport and assimilation. In root, a significant ($p < 0.01$) difference was observed in the expression patterns of the 5 tested nitrate and ammonium genes (*AtAMT1;1*, *AtAMT1;2*, *AtAMT1;3*, *AtNRT1;1* and *AtNRT2;2*) between deficient and sufficient N conditions (Figure 6b,e). Under low (0.25 mM) N treatment, a significant ($p < 0.01$) decrease was observed in OE lines versus wild-type except for *AtNRT1;1*, with a slight decrease, in contrast to a strongly upregulated expression in OE plants versus WT under sufficient (5 mM) N, except for a sharp decrease in the expression of *AtAMT1;3* and *AtNRT1;1* in OE plants. In leaves, both the amino acid transporters (*AtAAP1*, *AtAAP4*, *AtAAP5* and *AtAAP6*) and genes involved in N assimilation (the nitrate reductase encoding gene *AtNIA1*, the Gln synthetase encoding gene *AtGLN1;1* and Gln 2-oxoglutarate aminotransferase coding gene *AtGLU1*) were upregulated to different degrees under the two N conditions (Figure 6c,f). Specifically, under 0.25 mM N treatment, a strongly ($p < 0.01$) increased expression was observed in OE lines versus WT for all examined genes except for *AtAAP6*. Similarly, under 5 mM N treatment, a significantly ($p < 0.01$) elevated expression was found in OE lines for all the tested genes related to N transport and assimilation.

The aforementioned results indicate that the overexpression of *CsATG8e* in *Arabidopsis* could enhance the expression of autophagy-related genes, several amino acid transporters and genes related to N assimilation, regardless of the N condition. Meanwhile, the expressions of the genes related to N uptake all showed a decrease under low N stress, indicating the potential improvement of the N utilization capacity in transgenic plants. However, the mechanism for the improvement is different and depends on N conditions.

2.4.4. Transgenic Plants Increase Amino N

To evaluate the potential effect of *CsATG8e* on N remobilization during autophagy, we measured and compared the amino N levels between OE lines and WT plants. In Figure 7, the level of amino N was shown to increase in OE plants versus WT plants under the three N conditions, with a strikingly elevated concentration observed under the 1 mM N condition. The results indicate that the *CsATG8e* OE lines outperform the WT plants in amino N content in all the three N regimes from deficiency to sufficiency.

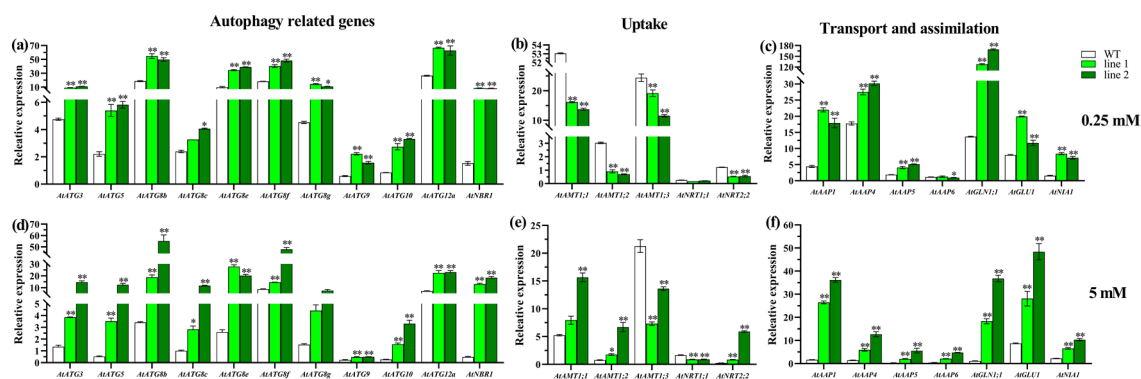


Figure 6. Gene expressions under deficient and sufficient N conditions. The expression of autophagy-related genes in leaves of overexpression *Arabidopsis* (OE) and wild-type (WT) plants under 0.25 mM (a) and 5 mM (d) N, respectively. The expression of the genes involved in N uptake in roots of OE and WT plants under 0.25 mM (b) and 5 mM (e) N, respectively. The expression of the genes related to N transport and assimilation in leaves of OE and WT plants under 0.25 mM (c) and 5 mM (f) N, respectively. 0.25 mM N, 0.125 mM NH₄NO₃; 5 mM N, 2.50 mM NH₄NO₃. Values are means ± standard (SD) (n = 3). Asterisks indicate significant difference between WT and two OE lines (line 1, line 2). * p < 0.05; ** p < 0.01 (t-test). AAP, amino acid permease gene; AMT, ammonium transporter; NRT, nitrate transporter; NIA, nitrate reductase encoding gene; GLU, Gln 2-oxoglutarate aminotransferase encoding gene; GLN, Gln synthetase encoding gene.

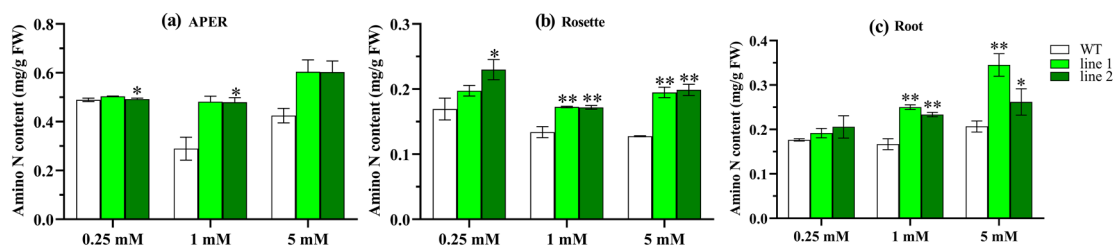


Figure 7. The content of amino N in overexpression *Arabidopsis* (OE) and wild type (WT). (a) The amino N content in aerial part excluding rosette (APER). (b) The amino N content in rosettes (Rosette). (c) The amino N content in roots (Root). 0.25 mM N, 0.125 mM NH₄NO₃; 1 mM N, 0.50 mM NH₄NO₃; 5 mM N, 2.50 mM NH₄NO₃. Values are means ± standard (SD) (n = 3). Asterisks indicate significant difference between WT and two OE lines (line 1, line 2). * p < 0.05; ** p < 0.01 (t-test).

2.4.5. Transgenic Plants Improve N Allocation in APER

Furthermore, we investigated how *CsATG8e* affects the distribution and accumulation of N under different N conditions. In APER, rosettes and roots, the N content in OE plants was shown to decrease dramatically relative to WT (Figure 8a) but varied with N conditions in the investigated parts (Supplementary Figure S2a–c). Generally, the N concentration increased with increasing N supply for all parts in OE lines and WT plants. When compared to WT plants, OE plants showed a decrease in the N concentration of rosettes and roots to a different degree under all three N conditions. However, in APER, the downregulated concentration of N was only observed under the 5 mM N condition, despite a non-statistical significance ($p > 0.05$). Additionally, we investigated the N allocation in APER (Figure 8b). Interestingly, the N allocation in APER was significantly increased in OE plants versus WT plants, indicating that *CsATG8e* could improve N allocation in APER independently of the N condition.

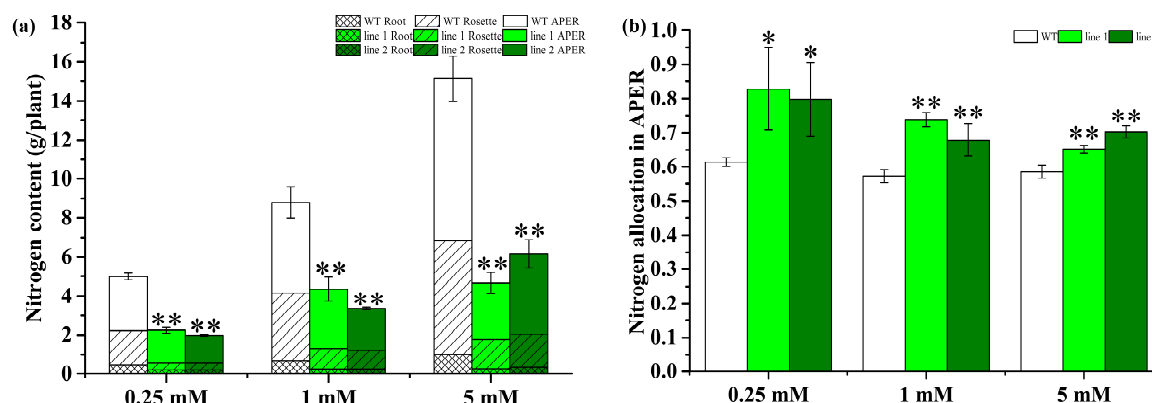


Figure 8. Analysis of N content and allocation in overexpression *Arabidopsis* (OE) and wild type (WT). (a) The N composition in OE lines and WT. (b) The N allocation in aerial part excluding rosette (APER). 0.25 mM N, 0.125 mM NH_4NO_3 ; 1 mM N, 0.50 mM NH_4NO_3 ; 5 mM N, 2.50 mM NH_4NO_3 . Values are means \pm standard (SD) ($n = 4$). Asterisks indicate significant difference between WT and two OE lines (line 1, line 2). * $p < 0.05$; ** $p < 0.01$ (t -test).

2.4.6. The Decrease in the Content of P and K in Transgenic Plants Is Mainly Attributed to Biomass Rather than the Concentration of P and K

Phosphorus (P) and potassium (K) are two other essential macronutrients in plants. To evaluate whether differences exist in the utilization efficiency of nutrients between OE lines and WT plants across the three tested N regimes, we determined the contents of P and K within plants (Supplementary Figure S3a,c). Under all three N conditions, the content of P and K showed a sharp decrease in OE lines versus WT in roots, rosettes and APER. A comparison between OE lines and WT (Supplementary Figure S2d–f) revealed no significant changes of P concentration in APER, while a significant increase in the rosettes of OE versus WT plants only under 1 mM N condition. In roots, the P concentration showed an increase in OE plants under all three N conditions, with a significantly ($p < 0.05$) higher P concentration observed at 1 and 5 mM N. As for K concentration, a similar downregulation was observed in the three parts of OE versus the WT plants under the 5 mM N condition (Supplementary Figure S2g–i). Under the 1 mM N condition, the K levels in OE plants showed a detectable ($p > 0.05$) increase in APER and roots and a decrease in rosettes when compared with WT.

Additionally, we calculated the P and K allocation in APER. Under the 1 mM N condition, the K allocation in APER showed a consistent increase in transgenic plants versus WT. These results suggest that it is the biomass rather than the concentration of P and K that contributes to the changes in the P and K allocation within the *CsATG8e* OE plants.

3. Discussion

ATG genes have been widely reported to participate in the autophagy process, an evolutionarily conserved intracellular process for balancing protein synthesis and degradation [34], and a number of *ATGs* have been identified in plants [8]. For example, in the model plant *Arabidopsis*, more than 40 *ATG* genes have been identified [18,25], and in other plants, 45 genes were identified in maize (*Zea mays*) [11], 33 in rice (*Oryza sativa*) [35], 30 in tobacco (*Nicotiana tabacum*) [36], 35 in grapevine (*Vitis vinifera*) [20] and 35 in sweet orange (*Citrus sinensis*) [37]. However, no *ATG* genes have been reported to be identified in tea plant yet. In the present study, a total of 80 *ATG* genes were identified in tea plant, a number obviously larger than that in other plants, nearly twice the number in *Arabidopsis*, which can be attributed to the following three reasons. Firstly, 24 subfamilies were found in the tea plant genomic database, which is more than the number in other plant species, such as 20 subfamilies in maize, 13 in rice, 16 in tobacco, 21 in grapevine and 19 in sweet orange [11,20,35–37]. Secondly, different methods were used to search for the homologues. In previous reports, BLASTN search or

keyword “autophagy” was applied, and in most cases, the sequences from *Arabidopsis* or/and rice were the only query-sequences [20,36,37]. In the present study, the query-sequences of *Arabidopsis* and another two woody plants were used to search for similar sequences. Finally, the improvement of genomic data for tea plant is still ongoing to obtain high-quality genomic data.

The identification of a large number of *ATG* members in tea plant implies the occurrence of duplication events of the *ATG* family, which was especially obvious for the subfamilies of *CsATG18*, *CsATG8* and *CsATG16*, whose total number occupies nearly half of all the identified *CsATG* members. Additionally, some of the *CsATG* genes share high similarity in a subfamily. For example, the two members (*CsATG8h* and *CsATG8i*) shared the same CDS with different gene structures and locations on chromosome (*CsATG8h* on chromosome 3 and *CsATG8i* on contig 424) (Figure 1a,b and Figure 3). For these genes, functional redundancy might be more frequently associated with their high similarity.

Unlike in yeast, the multiple members of a subfamily were usually observed for *ATG* genes in plants [17,38]. In our study, ten *ATG* genes were identified as a single copy in a separate subfamily. Among them, *ATG2* and *ATG5* are widely present as a single copy in higher plants, other than the genomic data we have mentioned above, which has also been proven in banana [39], pepper [40] and foxtail millet [41]. *ATG4* and *ATG9* are usually present as a single copy gene in many plants, such as tobacco [36], sweet orange [37], grapevine [20] and pepper [40], but with multiple members in a subfamily in rice [35]. In the present study, these genes were in small subfamilies with three and two members in *ATG4* and *ATG9*, respectively. Moreover, in higher plants, the subfamilies containing multiple members are always found in *ATG1*, *ATG8* and *ATG18* [8]. A similar result was found in tea plant for these subfamilies in the present study. Furthermore, we found that the members in a subfamily tend to share the same domains (Figure 3). In the subfamily of *CsATG18*, all members have the WD40 domain and seven members share an extra BCAS3 domain behind the WD40 domain, while in the *CsATG8* subfamily, ten of the members contain the Ubl_ATG8 domain and the other two have the Atg8 domain instead. Considering a closer distance in the phylogenetic trees (Figure 2), these results illustrated a closer relationship among the members with the similar conserved domains. Generally, the conserved domains and a relatively closer distance with woody species in the phylogenetic trees indicate a similarity in their functions, while separate branches and some tightly clustered members in tea plant suggest that some genes might be either in neofunctionalization or in redundancy.

In the species of *Arabidopsis* and rice, the functions of *ATG8* subfamily members are shown to be involved in the utilization of nutrients, especially N [27,28,42]. Previous studies have confirmed that autophagy occurs at a very low level under normal conditions, while it is stimulated during senescence or in stressful conditions [43,44]. In this study, the expressions of 10 members in *CsATG8s* from the three tea cultivars mostly showed the highest expression at S4, while the lowest at S1 (Figure 4a), where the S4 leaves represented ageing leaves, while S1 tissues were young developing leaves with the requirement of a significant amount of nutrient for their growth and development, which can serve as supplementary to the previous results. Because of the central role of *ATG8* in autophagy, the expression patterns of *CsATG8s* in the four types of leaves from the three tea cultivars indicated that autophagy plays an important role in tea plant, implying the substrate remobilization from S4 to S1. However, the non-uniform expression patterns of the 10 *CsATG8s* indicated that they may have different functions or work at different occasions in tea plants. Additionally, the obvious upward tendency in the expression of *CsATG8e* from S1 to S4 suggested a specific function of this gene in nutrient redistribution in tea plant.

N has been demonstrated as one of the efficient contributors to stimulate autophagy [28,45]. In our study, we demonstrated that the expressions of sixteen genes were highly upregulated by N stimuli, especially under the sufficient N condition (5 mM N). However, previous studies have shown that autophagy can be more easily induced by nutrient starvation [46]. This discrepancy in results might be due to the different states of plants before N treatment in previous studies, where the plants were cultured in the sufficient N condition, while in our experiment, plants were subjected to ten days of N starvation. Additionally, the increased expression levels under both deficient and sufficient N

conditions, especially in mature leaves, indicated that the autophagy process plays an important role in N economy within tea plant. Furthermore, the transcript levels of *CsATG8e* were found to change greatly within treatments, indicating an intimate connection of *CsATG8e* with N in tea plant.

The important role of autophagy in nutrient recycling has been proved in *Arabidopsis* [47,48]. In crops like rice [42,49,50] and soybean [51], a number of members in the ATG8 subfamily have been shown to participate in N utilization. Previous studies have shown that the ATG9 complex and ubiquitin-like conjugation pathways are indispensable in the process of autophagy and NBR1 is a typical receptor for selective autophagy [25,33]. In this study, the expressions of *AtATG9*, *AtNBR1* and 9 genes in ubiquitin-like conjugation pathways were found to be upregulated in OE lines versus WT (Figure 6a,d), indicating the enhanced autophagy in *CsATG8e* transgenic plants. As reported in earlier studies, *AtNRT1;1* and *AtNRT2;2* showed low and high affinity for nitrate uptake respectively, and *AtAMT1;1*, *AtAMT1;2* and *AtAMT1;3* absorbed up to 95% of ammonium in *Arabidopsis*, which are the major genes related to N uptake in *Arabidopsis* [52]. In this study, the expression of most of these genes in OE plants were downregulated under the 0.25 mM N condition and upregulated under the 5 mM N condition compared with WT (Figure 6b,e), indicating the occurrence of a different mechanism for *CsATG8e*-overexpressed plants under different N levels. *AAP1*, *AAP4*, *AAP5* and *AAP6* have been confirmed to play important roles in the transport of amino acids, while *AtNIA1*, *AtGLN1;1* and *AtGLU1* are members involved in N assimilation [53,54]. In our study, the upregulated expression of these genes in transgenic plants versus control plants (Figure 6c,f) demonstrated the enhancement of N utilization in *CsATG8e*-overexpressed plants.

Moreover, we demonstrated that compared with WT, the OE lines showed an earlier reproductive stage and senescence, a decrease in biomass and the content of N, P and K, while an increase in amino N. The increase of amino acid level has been shown to result from proteolysis for reuse in plants via autophagy [9]. Clearly, the higher amino N level in OE lines can be attributed to the degradation of severely senescent leaves. The earlier productive stage has been reported in soybean [55] and rice [42]. However, the results of biomass and nutrient content in the present study were inconsistent with those of *SiATG8a* [41], *OsATG8a* [50] and *MdATG8i* [26], in which the transgenic plants showed better growth and accumulated more N, whereas a recent study has demonstrated that the overexpression of *ATG8* in *Arabidopsis* has no effect on vegetative biomass or plant development [28]. In general, the tea plant is a woody plant with new vegetative organs rather than reproductive organs as economic products. Here, we investigated the nutrient allocation in the APER of *Arabidopsis* before the plants entered the mature reproductive stage, and the OE plants were shown to have an increase over the WT plants in the allocation of biomass and the content of N, P and K, with a slight difference between them in the concentration of N, P and K, indicating that the nutrient content mainly comes from biomass. These findings suggest that *CsATG8e* performs a potential function in the allocation of nutrients or the development of plants.

4. Materials and Methods

4.1. Identification of *CsATG* Genes

To comprehensively identify the ATG superfamily members in tea plant, the genomes of *Arabidopsis thaliana* (<https://www.Arabidopsis.org/>) and *Camellia sinensis* in CSS_ChrLev_20200506 version (<http://tpia.teaplant.org/index.html>) [23] were first compared by BLASTp at the whole genomic level under E-values above 1×10^{-5} . Next, 49 autophagy-related gene proteins (ATGs) from *Arabidopsis thaliana* were used to acquire the corresponding proteins in *Camellia sinensis*. Simultaneously, 37 and 35 autophagy-related protein sequences from *Citrus sinensis* (<http://citrus.hzau.edu.cn/orange/>) and *Vitis vinifera* (<http://plants.ensembl.org/index.html>) were used in a BLASTp search for the similar sequences in *Camellia sinensis* genome under E-values above 1×10^{-5} . Based on the sequences from the above three BLASTp searches, another BLASTp search was performed in NCBI (National Center for Biotechnology Information, <https://blast.ncbi.nlm.nih.gov/Blast.cgi>) to ensure that the sequences were

annotated as autophagy-related genes, and the conserved domains were further validated online in the NCBI Conserved Domain Database (<https://www.ncbi.nlm.nih.gov/cdd/>) according to the domains from *Arabidopsis* (Supplementary Table S3). The isoelectric point (PI) and molecular weight (MW) were calculated by the ExPASy website (https://web.expasy.org/compute_pi/). TBtools [56] was used to acquire the sequences from tea genome and analyze the length of genes.

4.2. Phylogenetic Tree Construction and Analysis of Conserved Motif and Gene Structure of CsATGs

To investigate the evolutionary relationship of the CsATGs and homologues with those of other plant species, neighbor-joining phylogenetic trees were constructed respectively based on the subfamily of CsATG proteins together with three other species, *Arabidopsis thaliana* (At) from TAIR (The Arabidopsis Information Resource, <https://www.Arabidopsis.org/>), *Vitis vinifera* (Vv) from Ensemble Plants (<http://plants.ensembl.org/index.html>) and *Citrus sinensis* (Cis) from the sweet orange genome database (<http://citrus.hzau.edu.cn/orange/>), with their corresponding Gene Bank accession numbers listed in Supplementary Table S4. MEGA-X (<http://www.megasoftware.net>) was first used to align the amino acid sequences and generate the unrooted phylogenetic tree by the neighbor-joining method with 1000 repetitions. The online tool iTOL (<https://itol.embl.de/>) was used to visualize the phylogenetic trees. The conserved motifs and domains were analyzed using MEME (Multiple Em for Motif Elicitation, <http://alternate.meme-suite.org/tools/meme>) and NCBI-CDD (Conserved Domain Database, <https://www.ncbi.nlm.nih.gov/Structure/bwrpsb/bwrpsb.cgi>) and visualized with TBtools. The exon-intron structures of the CsATGs were determined by comparing the coding sequences (CDS) with the corresponding genomic sequences using Gene Structure Display Server (GSDS, <https://www.ncbi.nlm.nih.gov/cdd>).

4.3. Plant Materials and Nitrogen Treatments

To examine the expression of CsATG8s in tea leaves at different development stages, leaves at four different growing phases, including one bud with two leaves or the same tenderness with two leaves near the bud that stops growing (Stage 1, S1), leaves attached to the red and green stems (Stage 2, S2), leaves attached to the gray stems (Stage 3, S3) and ageing leaves with a tendency to become yellow (Stage 4, S4), were collected on 28 September 2017 from tea plants of three different green tea cultivars in the Tea Plantation of HuaZhong Agricultural University (Wuhan, Hubei, China). The tea cultivars included *Fuding Dabai* and *Echa 10*, two national cultivars largely grown in China, and *Zhongcha 108*, a provincial cultivar mainly grown in Hubei province. The leaves with a similar and vigorous growth status were used in the experiments. All samples were collected and frozen immediately in liquid nitrogen and stored at $-80\text{ }^{\circ}\text{C}$ for RNA extraction.

To reveal the response of ATGs to different N regimes, *Zhongcha 108* was used to examine the expression profiles. The two-year-old cutting seedlings were planted in the plastic basin (48 plants per basin) containing 7 L of hydroponic culture in a chamber ($22\text{ }^{\circ}\text{C}/18\text{ }^{\circ}\text{C}$, 16 h light/8 h dark) for 15 days. The concentration of the nutrient solution was refreshed every five days, stepwise supplied at 1/8 to 1/4 and then 1/2 strength. Finally, the plants were cultured with full-strength solution for another two months until the new roots developed. For the N treatment, plants were first cultured in the solution without N for ten days, followed by exposure to the solution containing N at 0.25 mM (deficient, 0.125 mM NH_4NO_3), or 5.0 mM (sufficient, 2.50 mM NH_4NO_3) for 8 h. The samples of young leaves and mature leaves were collected and frozen immediately in $-80\text{ }^{\circ}\text{C}$ for RNA extraction, and the samples collected before the 8 h treatment were used as the control (CK). Here, the full-strength solution was based on Wan et al. [57] with slight changes, which contained 2.50 mM NH_4NO_3 , 1 mM KH_2PO_4 , 0.15 mM K_2SO_4 , 0.44 mM $\text{CaCl}_2\cdot 2\text{H}_2\text{O}$, 0.43 mM $\text{MgSO}_4\cdot 7\text{H}_2\text{O}$, 0.125 mM $\text{Al}_2(\text{SO}_4)_3\cdot 18\text{H}_2\text{O}$, 2.1 μM Na_2EDTA , 2.1 μM $\text{FeSO}_4\cdot 7\text{H}_2\text{O}$, 3.33 μM H_3BO_3 , 0.50 μM $\text{MnSO}_4\cdot \text{H}_2\text{O}$, 0.51 μM $\text{ZnSO}_4\cdot 7\text{H}_2\text{O}$, 0.13 μM $\text{CuSO}_4\cdot 5\text{H}_2\text{O}$, and 0.17 μM $\text{Na}_2\text{MoO}_4\cdot 2\text{H}_2\text{O}$, with pH 5.83 for the solution.

OE *Arabidopsis* plants were cultured in the soil in a growth chamber ($22\text{ }^{\circ}\text{C}/18\text{ }^{\circ}\text{C}$, 16 h light/8 h dark) to obtain homozygous T3 seeds. To investigate the N patterns mediated by CsATG8e, wild type

(WT, Col-0) and two homozygous T3 lines with relatively higher expression levels were used to compare their growth, N level and allocation in response to the three different N regimes. Firstly, the seeds were surface-sterilized and sowed on plates containing 1/2 MS (Murashige and Skoog) medium (with 1% agar and 1% sucrose (w:v), pH = 5.83), then stratified at 4 °C for two days in the dark, and finally grown in a growth chamber (22 ± 1 °C and 16 h light/8 h dark) for two weeks. Next, the plants were transferred to fresh 1/2 modified Hoagland's solution for 5 days, followed by culture for another 15 days in the full Hoagland's solution, which contained 2.50 mM NH₄NO₃, 1.6 mM CaCl₂·2H₂O, 0.4 mM K₂HPO₄·3H₂O, 0.7 mM K₂SO₄, 1 mM MgSO₄·7H₂O, 25 μM FeSO₄·7H₂O, 25 μM Na₂EDTA, 9 μM MnSO₄·H₂O, 47 μM H₃BO₃, 0.8 μM ZnSO₄·7H₂O, 0.3 μM CuSO₄·5H₂O and 0.1 μM Na₂MoO₄·2H₂O, with the full solution renewed every 5 days. Subsequently, the N in the solutions was replaced with low (0.25 mM N, 0.125 mM NH₄NO₃), moderate (1 mM N, 0.50 mM NH₄NO₃) and high (5 mM N, 2.50 mM NH₄NO₃) levels separately for another 14 days of culture, with each of the solutions renewed once a week until the samples were collected. Twenty days after transferring from plates, the grown plants were recorded for the first time and then treated with the three different N regimes as described above. One week after such treatments, samples of roots and leaves under low and high conditions were collected from at least three plants for gene expression analysis. Finally, at the end of the cultivation, the plants were photographed again and then sampled by separation into Root, Rosette and APER for measurement of biomass and N, P and K concentration.

4.4. RNA Extraction and Gene Expression Analysis

Total RNA was extracted from tea leaves, *Arabidopsis* leaves and respective roots using the Quick RNA Isolation Kit according to the manufacturer's protocol (Huayueyang, Beijing, China). The RNA was treated with gDNA Eraser to remove DNA contaminants (Aidlab, Beijing, China). Reverse transcription was performed using TRUEScript RT Kit (Aidlab, Beijing, China) with 1 μg RNA. The resulting cDNAs were diluted at 1:10 with ddH₂O, and qRT-PCR was performed using an ABI StepOnePlus Real-Time PCR System (Applied Biosystems) with SYBR Green qPCR Mix (Aidlab, Beijing, China) following a recommended protocol. Fold changes in gene expression were calculated by comparing the C_T values using the 2^{-ΔΔ} method [58] with the internal control genes of *CsGAPDH* for *Camellia sinensis* and *AtGAPDH* for *Arabidopsis*. Three biological replicates were performed, and each replicate was collected from at least two independently grown sets of plants. Accession numbers and primer sequences are shown in Supplementary Table S5.

4.5. Cloning of *CsATG8e* and Generation of Transgenic *Arabidopsis thaliana* Plants

The ORF of *CsATG8* was firstly amplified with non-restriction enzyme primers from cDNA of *Fudingdabai* cultivar and cloned into pTOPO vector following the manufacturer's instructions. After sequencing and alignment against the reference genome, the confirmed coding sequences were separately amplified with primers containing *Xba* I/*Xho* I and finally inserted into pBin35SRed [59]. The resulting constructs were introduced into *Agrobacterium tumefaciens* strain GV3101. Finally, transformation of *Arabidopsis thaliana* wild type was performed using the floral dip method [60]. Two independently homozygous T3 lines with *CsATG8e* at the high expression level were selected for further analysis. All primers used in vector construction are shown in Supplementary Table S5.

4.6. Determination of N, P and K Concentration and Amino N in *Arabidopsis*

Samples of Root, Rosette and APER were oven-dried at 120 °C for 10 min, followed by 75 °C for 5 days to a constant weight. Biomass was calculated as the sum of dry weights from the separated parts. To measure the total N, P and K concentration, the dried samples were firstly ground into fine powder, followed by digestion with H₂SO₄-H₂O₂. The concentrations of N and P were determined simultaneously using a flow injection analysis instrument (FIAstar 5000 analyzer; FOSS, Hilleroed, Denmark). The concentration of K was determined with a flame spectrophotometer (Sherwood M410).

To measure the amount of amino N, fresh samples (~0.15 g) of Root, Rosette and APER were weighed separately, followed by measuring the amount of amino N with the Ninhydrin Colorimetric Analysis method [61].

4.7. Statistical Analysis

For each determination, at least three independent replicates were carried out. Data were presented as mean \pm standard deviation. OE lines and WT were statistically analyzed by Student's *t*-test at significance levels of * $p < 0.05$ and ** $p < 0.01$ using the SPSS 21.0 software (IBM, Chicago, IL, USA). Significant differences in tea plant were indicated with lowercase letters using analysis of variance (ANOVA) Duncan's test at $p < 0.05$ or $p < 0.01$. All the figures were drawn using the software of OriginPro 9.1 (OriginLab, Northampton, MA, USA) or TBtools and Adobe illustrator CC2019 (ADOBE, San Jose, CA, USA).

Supplementary Materials: Supplementary Materials can be found at <http://www.mdpi.com/1422-0067/21/19/7043/s1>. Table S1. The sequence characteristics of CsATG genes in tea plant. Table S2. Molecular evolutionary rate of duplicated CsATG pairs in tea plant. Table S3. ATG domains for AtATGs in *Arabidopsis thaliana*. Table S4. List of genes and protein sequences used in this study. Table S5. Primer sequences used in this study. Figure S1. Amino acid sequence alignment of CsATG8e and ATG8 members in *Arabidopsis* and tea plant. Figure S2. The concentration of N, P and K in overexpression *Arabidopsis* (OE) and wild type (WT) under three N regimes. Figure S3. Analysis of P and K content and allocation in overexpression *Arabidopsis* (OE) and wild type (WT).

Author Contributions: W.H., P.W. and H.Z. conceived and designed the study; W.H. and J.L. performed bioinformatic analysis; D.-N.M. and H.-L.L. performed N treatments on tea plant; H.-L.L., D.-N.M. and W.H. measured the concentration of N, P and K; D.-N.M. and W.H. conducted the other experiments; J.L. visualized, revised and edited the manuscript; D.-J.N., M.-L.W., F.G. and Y.W. reviewed the manuscript and gave some suggestions; H.Z. performed funding acquisition, validation, visualization, project administration, critical revision and manuscript editing; W.H. prepared all of the figures and tables and wrote the manuscript. All authors have read and agreed to the published version of the manuscript.

Funding: This research was founded by the National Key Research and Development Program of China (2018YFD1000600), the National Natural Science Foundation of China (32070376) and the Fundamental Research Funds for the Central Universities of China (2662018JC046).

Conflicts of Interest: The authors declare no conflict of interest.

Abbreviations

APER	aerial part excluding rosette
ATG	autophagy-related gene
AAP	amino acid permease gene
AMT	ammonium transporter
NRT	nitrate transporter
NIA	nitrate reductase encoding gene
GLU	Gln 2-oxoglutarate aminotransferase encoding gene
GLN	Gln synthetase encoding gene
OE	overexpression
WT	wild type
ORF	open reading frame
UTR	untranslated region
ATG_C	Autophagy-related protein C terminal domain
Chorein_N	N-terminal region of Chorein
Autophagy_N	Autophagocytosis-associated protein N-terminus
Autophagy_C	Autophagocytosis-associated protein C-terminus
Autophagy_act_C	Autophagocytosis-associated protein, active-site domain
Peptidase_C54	Peptidase family C54
E1_like_apg7	E1-like protein-activating enzyme Gsa7p/Apg7p
Ubl_ATG8	ubiquitin-like (Ubl) domain and sub-family of the autophagy-related 8 family
Ubl_ATG12	ubiquitin-like domain found in autophagy-related protein 12

WD40	WD40 repeat
BCAS3	Breast carcinoma amplified sequence 3
PX_SNX1_2_like	Phosphoinositide binding Phox Homology domain of Sorting Nexins 1 and 2
BAR_SNK	Bin/Amphiphysin/Rvs (BAR) domain of Sorting Nexins
C2_PI3K_class_III	C2 domain present in class III phosphatidylinositol 3-kinases
PI3Ka_III	Phosphoinositide 3-kinase class III
PI3Kc_III	Catalytic domain of Class III Phosphoinositide 3-kinase
Vps35	Vacuolar protein sorting-associated protein 35
NBR1_like	neighbor of Brca1 Gene 1 and related proteins
UBA_NBR1	UBA domain of next to BRCA1 gene 1 protein (NBR1) and similar proteins
ZZ superfamily	Zinc finger, ZZ type
V-SNARE	Vesicle transport v-SNARE protein N-terminus
SNARE_Vti1	SNARE motif of Vti1
PKc-like	Protein Kinases, catalytic domain
STKc_ATG1_ULK_like	Catalytic domain of the Serine/Threonine kinases, Autophagy-related protein 1 and Unc-51-like kinases
STKc_Vps15	Catalytic domain of the Serine/Threonine kinase, Vacuolar protein sorting-associated protein 15

References

- Mukhopadhyay, M.; Mondal, T.K.; Chand, P.K. Biotechnological advances in tea (*Camellia sinensis* [L.] O. Kuntze): A review. *Plant Cell Rep.* **2016**, *35*, 255–287. [[CrossRef](#)] [[PubMed](#)]
- Chen, L.; Apostolides, Z.; Chen, Z.M. *Global Tea Breeding, Achievements, Challenges and Perspectives*; Springer-Zhejiang University Press: Hangzhou, China, 2012.
- Bouwman, A.F.; Boumans, L.J.M.; Batjes, N. Emissions of N₂O and NO from fertilized fields: Summary of available measurement data. *Glob. Biogeochem. Cycles* **2002**, *16*, 1058. [[CrossRef](#)]
- Gruber, N.; Galloway, J.N. An Earth-system perspective of the global nitrogen cycle. *Nature* **2008**, *451*, 293–296. [[CrossRef](#)]
- Maegan, A.G.; Rakesh, M.; Stephanie, L.; Subhash, C.M. Effects of different foliar nitrogen fertilizers on cellular nitrogen metabolism and biomass of two shrub willow cultivars. *NRC Res. Press* **2019**, *49*, 1548–1559.
- Alessandro, M.; Pasquale, S.; Antonio, D.; Daniela, S.; Giuseppe, C.; Youssef, R.; Boris, B. Foliar application of an amino acid-enriched urea fertilizer on ‘Greco’ grapevines at full veraison increases berry yeast-assimilable nitrogen content. *Plants* **2020**, *9*, 619.
- Fan, K.; Zhang, Q.; Liu, M.Y.; Ma, L.; Shi, Y.; Ruan, J. Metabolomic and transcriptional analyses reveal the mechanism of C, N allocation from source leaf to flower in tea plant (*Camellia sinensis* L.). *J. Plant Physiol.* **2019**, *232*, 200–208. [[CrossRef](#)] [[PubMed](#)]
- Masclaux-Daubresse, C.; Chen, Q.; Havé, M. Regulation of nutrient recycling via autophagy. *Curr. Opin. Plant Biol.* **2017**, *39*, 8–17. [[CrossRef](#)]
- Liu, Y.; Bassham, D.C. Autophagy: Pathways for self-eating in plant cells. *Annu. Rev. Plant Biol.* **2012**, *63*, 215–237. [[CrossRef](#)]
- Hanaoka, H.; Noda, T.; Shirano, Y.; Kato, T.; Hayashi, H.; Shibata, D.; Tabata, S.; Ohsumi, Y. Leaf senescence and starvation-induced chlorosis are accelerated by the disruption of an arabidopsis autophagy gene. *Plant Physiol.* **2002**, *129*, 1181–1193. [[CrossRef](#)]
- Li, F.; Chung, T.; Pennington, J.G.; Federico, M.L.; Kaeppler, H.F.; Kaeppler, S.; Otegui, M.S.; Vierstra, R.D. Autophagic recycling plays a central role in maize nitrogen remobilization. *Plant Cell* **2015**, *27*, 1389–1408. [[CrossRef](#)]
- Masclaux-Daubresse, C.; Reisdorf-Cren, M.; Orsel, M. Leaf nitrogen remobilization for plant development and grain filling. *Plant Biol.* **2008**, *10*, 23–36. [[CrossRef](#)] [[PubMed](#)]
- Diaz, C.; Lemaître, T.; Christ, A.; Azzopardi, M.; Kato, Y.; Sato, F.; Morot-Gaudry, J.F.; Le Dily, F.; Masclaux-Daubresse, C. Nitrogen recycling and remobilization are differentially controlled by leaf senescence and development stage in arabidopsis under low nitrogen nutrition. *Plant Physiol.* **2008**, *147*, 1437–1449. [[CrossRef](#)] [[PubMed](#)]

14. Wada, S.; Hayashida, Y.; Izumi, M.; Kurusu, T.; Hanamata, S.; Kanno, K.; Kojima, S.; Yamaya, T.; Kuchitsu, K.; Makino, A.; et al. Autophagy supports biomass production and nitrogen use efficiency at the vegetative stage in rice. *Plant Physiol.* **2015**, *168*, 60–73. [[CrossRef](#)]
15. Guiboileau, A.; Yoshimoto, K.; Soulay, F.; Bataillé, M.P.; Avice, J.C.; Masclaux-Daubresse, C. Autophagy machinery controls nitrogen remobilization at the whole-plant level under both limiting and ample nitrate conditions in Arabidopsis. *New Phytol.* **2012**, *194*, 732–740. [[CrossRef](#)] [[PubMed](#)]
16. Tsukada, M.; Ohsumi, Y. Isolation and characterization of autophagy-defective mutants of *Saccharomyces cerevisiae*. *FEBS Lett.* **1993**, *333*, 169–174. [[CrossRef](#)]
17. Avila-Ospina, L.; Moison, M.; Yoshimoto, K.; Masclaux-Daubresse, C. Autophagy, plant senescence, and nutrient recycling. *J. Exp. Bot.* **2014**, *65*, 3799–3811. [[CrossRef](#)]
18. Han, S.; Yu, B.; Wang, Y.; Liu, Y. Role of plant autophagy in stress response. *Protein Cell* **2011**, *2*, 784–791. [[CrossRef](#)]
19. Li, F.; Chung, T.; Vierstra, R.D. AUTOPHAGY-RELATED₁₁ Plays a Critical Role in General Autophagy- and Senescence-Induced Mitophagy in Arabidopsis. *Plant Cell* **2014**, *26*, 788–807. [[CrossRef](#)]
20. Shangguan, L.; Fang, X.; Chen, L.; Cui, L.; Fang, J. Genome-wide analysis of autophagy-related genes (ARGs) in grapevine and plant tolerance to copper stress. *Planta* **2018**, *247*, 1449–1463. [[CrossRef](#)]
21. Xia, E.H.; Zhang, H.B.; Sheng, J.; Li, K.; Zhang, Q.J.; Kim, C.; Zhang, Y.; Liu, Y.; Zhu, T.; Li, W.; et al. The tea tree genome provides insights into tea flavor and independent evolution of caffeine biosynthesis. *Mol. Plant* **2017**, *10*, 866–877. [[CrossRef](#)] [[PubMed](#)]
22. Zhang, W.; Zhang, Y.; Qiu, H.; Guo, Y.; Wan, H.; Zhang, X.; Scossa, F.; Alseekh, S.; Zhang, Q.; Wang, P.; et al. Genome assembly of wild tea tree DASZ reveals pedigree and selection history of tea varieties. *Nat. Commun.* **2020**, *11*, 3719. [[CrossRef](#)]
23. Xia, E.H.; Li, F.; Tong, W.; Li, P.; Wu, Q.; Zhao, H.; Ge, R.H.; Li, R.; Li, Y.; Zhang, Z.; et al. Tea Plant Information Archive: A comprehensive genomics and bioinformatics platform for tea plant. *Plant Biotechnol. J.* **2019**, *17*, 1938–1953. [[CrossRef](#)] [[PubMed](#)]
24. Li, F.; Vierstra, R.D. Autophagy: A multifaceted intracellular system for bulk and selective recycling. *Trends Plant Sci.* **2012**, *17*, 526–537. [[CrossRef](#)] [[PubMed](#)]
25. Kwon, S.I.; Park, O.K. Autophagy in plants. *J. Plant Biol.* **2008**, *51*, 313–320. [[CrossRef](#)]
26. Wang, P.; Sun, X.; Jia, X.; Wang, N.; Gong, X.; Ma, F. Characterization of an autophagy-related gene MdATG8i from apple. *Front. Plant Sci.* **2016**, *7*, 720. [[CrossRef](#)] [[PubMed](#)]
27. Zhen, X.; Li, X.; Yu, J.; Xu, F. OsATG8c-mediated increased autophagy regulates the yield and nitrogen use efficiency in rice. *Int. J. Mol. Sci.* **2019**, *20*, 4956. [[CrossRef](#)] [[PubMed](#)]
28. Chen, Q.; Soulay, F.; Saudemont, B.; Elmayan, T.; Marmagne, A.; Masclaux-Daubresse, C.; Masclaux-Daubresse, C. Overexpression of ATG8 in Arabidopsis stimulates autophagic activity and increases nitrogen remobilization efficiency and grain filling. *Plant Cell Physiol.* **2019**, *60*, 343–352. [[CrossRef](#)]
29. Lornac, A.; Havé, M.; Chardon, F.; Soulay, F.; Clément, G.; Avice, J.-C.; Masclaux-Daubresse, C. Autophagy controls sulphur metabolism in the rosette leaves of Arabidopsis and facilitates S remobilization to the seeds. *Cells* **2020**, *9*, 332. [[CrossRef](#)]
30. Pottier, M.; Dumont, J.; Masclaux-Daubresse, C.; Thomine, S. Autophagy is essential for optimal translocation of iron to seeds in Arabidopsis. *J. Exp. Bot.* **2019**, *70*, 859–869. [[CrossRef](#)]
31. Pottier, M.; Masclaux-Daubresse, C.; Yoshimoto, K.; Thomine, S. Autophagy as a possible mechanism for micronutrient remobilization from leaves to seeds. *Front. Plant Sci.* **2014**, *5*, 11. [[CrossRef](#)]
32. Wu, W.; Liu, Y.; Wang, Y.; Li, H.; Liu, J.; Tan, J.; He, J.; Bai, J.; Ma, H. Evolution analysis of the Aux/IAA gene family in plants shows dual origins and variable nuclear localization signals. *Int. J. Mol. Sci.* **2017**, *18*, 2107. [[CrossRef](#)]
33. Bu, F.; Yang, M.; Guo, X.; Huang, W.; Chen, L. Multiple functions of ATG8 family proteins in plant autophagy. *Front. Cell Dev. Biol.* **2020**, *8*, 466. [[CrossRef](#)] [[PubMed](#)]
34. Kim, S.H.; Kwon, C.; Lee, J.H.; Chung, T. Genes for plant autophagy: Functions and interactions. *Mol. Cells* **2012**, *34*, 413–423. [[CrossRef](#)]
35. Xia, K.; Liu, T.; Ouyang, J.; Wang, R.; Fan, T.; Zhang, M. Genome-wide identification, classification, and expression analysis of autophagy-associated gene homologues in rice (*Oryza sativa* L.). *DNA Res.* **2011**, *18*, 363–377. [[CrossRef](#)] [[PubMed](#)]

36. Zhou, X.M.; Zhao, P.; Wang, W.; Zou, J.; Cheng, T.H.; Peng, X.B.; Sun, M.X. A comprehensive, genome-wide analysis of autophagy-related genes identified in tobacco suggests a central role of autophagy in plant response to various environmental cues. *DNA Res.* **2015**, *22*, 245–257. [[CrossRef](#)]
37. Fu, X.Z.; Zhou, X.; Xu, Y.Y.; Hui, Q.L.; Chang-Pin, C.; Li-Li, L.; Liang-Zhi, P. Comprehensive analysis of autophagy-related genes in sweet orange (*Citrus sinensis*) highlights their roles in response to abiotic stresses. *Int. J. Mol. Sci.* **2020**, *21*, 2699. [[CrossRef](#)]
38. Thompson, A.R.; Vierstra, R.D. Autophagic recycling: Lessons from yeast help define the process in plants. *Curr. Opin. Plant Biol.* **2005**, *8*, 165–173. [[CrossRef](#)]
39. Wei, Y.; Liu, W.; Hu, W.; Liu, G.; Wu, C.; Liu, W.; Zeng, H.; He, C.; Shi, H. Genome-wide analysis of autophagy-related genes in banana highlights MaATG8s in cell death and autophagy in immune response to Fusarium wilt. *Plant Cell Rep.* **2017**, *36*, 1237–1250. [[CrossRef](#)]
40. Zhai, Y.; Guo, M.; Wang, H.; Lu, J.; Liu, J.; Zhang, C.; Gong, Z.; Lu, M. Autophagy, a conserved mechanism for protein degradation, responds to heat, and other abiotic stresses in *Capsicum annuum* L. *Front. Plant Sci.* **2016**, *7*, 131. [[CrossRef](#)]
41. Li, W.; Chen, M.; Wang, E.; Hu, L.; Hawkesford, M.J.; Zhong, L.; Chen, Z.; Xu, Z.; Li, L.; Zhou, Y.; et al. Genome-wide analysis of autophagy-associated genes in foxtail millet (*Setaria italica* L.) and characterization of the function of SiATG8a in conferring tolerance to nitrogen starvation in rice. *BMC Genom.* **2016**, *17*, 797. [[CrossRef](#)]
42. Zhen, X.; Xu, F.; Zhang, W.; Li, N.; Li, X. Overexpression of rice gene OsATG8b confers tolerance to nitrogen starvation and increases yield and nitrogen use efficiency (NUE) in Arabidopsis. *PLoS ONE* **2019**, *14*, e0223011. [[CrossRef](#)] [[PubMed](#)]
43. Wang, P.; Mugume, Y.; Bassham, D.C. New advances in autophagy in plants: Regulation, selectivity and function. *Semin. Cell Dev. Biol.* **2018**, *80*, 113–122. [[CrossRef](#)] [[PubMed](#)]
44. Himelblau, E.; Amasino, R.M. Nutrients mobilized from leaves of Arabidopsis thaliana during leaf senescence. *J. Plant Physiol.* **2001**, *158*, 1317–1323. [[CrossRef](#)]
45. An, Z.Y.; Tassa, A.; Thomas, C.; Zhong, R.; Xiao, G.H.; Fotedar, R.; Tu, B.P.; Klionsky, D.J.; Levine, B. Autophagy is required for G1/G0 quiescence in response to nitrogen starvation in *Saccharomyces cerevisiae*. *Autophagy* **2014**, *10*, 1702–1711.
46. Onodera, J.; Ohsumi, Y. Autophagy is required for maintenance of amino acid levels and protein synthesis under nitrogen starvation. *J. Biol. Chem.* **2005**, *280*, 31582–31586. [[CrossRef](#)]
47. Di Berardino, J.; Marmagne, A.; Berger, A.; Yoshimoto, K.; Cueff, G.; Chardon, F.; Masclaux-Daubresse, C.; Reisdorf-Cren, M. Autophagy controls resource allocation and protein storage accumulation in Arabidopsis seeds. *J. Exp. Bot.* **2018**, *69*, 1403–1414. [[CrossRef](#)]
48. Guiboileau, A.; Avila-Ospina, L.; Yoshimoto, K.; Soulay, F.; Azzopardi, M.; Marmagne, A.; Lothier, J.; Masclaux-Daubresse, C. Physiological and metabolic consequences of autophagy deficiency for the management of nitrogen and protein resources in Arabidopsis leaves depending on nitrate availability. *New Phytol.* **2013**, *199*, 683–694. [[CrossRef](#)]
49. Fan, T.; Yang, W.; Zeng, X.; Xu, X.; Xu, Y.; Fan, X.; Luo, M.; Tian, C.; Xia, K.; Zhang, M. A rice autophagy gene OsATG8b is involved in nitrogen remobilization and control of grain quality. *Front. Plant Sci.* **2020**, *11*, 588. [[CrossRef](#)]
50. Yu, J.; Zhen, X.; Li, X.; Li, N.; Xu, F. Increased autophagy of rice can increase yield and nitrogen use efficiency (NUE). *Front. Plant Sci.* **2019**, *10*, 584. [[CrossRef](#)]
51. Islam, M.; Ishibashi, Y.; Nakagawa, A.C.; Tomita, Y.; Iwaya-Inoue, M.; Arima, S.; Zheng, S.-H. Nitrogen redistribution and its relationship with the expression of GmATG8c during seed filling in soybean. *J. Plant Physiol.* **2016**, *192*, 71–74. [[CrossRef](#)]
52. Tegeder, M.; Masclaux-Daubresse, C. Source and sink mechanisms of nitrogen transport and use. *New Phytol.* **2018**, *217*, 35–53. [[CrossRef](#)] [[PubMed](#)]
53. Tegeder, M. Transporters for amino acids in plant cells: Some functions and many unknowns. *Curr. Opin. Plant Biol.* **2012**, *15*, 315–321. [[CrossRef](#)]
54. Santiago, J.P.; Tegeder, M. Connecting source with sink: The role of arabidopsis AAP8 in phloem loading of amino Acids. *Plant Physiol.* **2016**, *171*, 508–521. [[CrossRef](#)] [[PubMed](#)]

55. Xia, T.; Xiao, D.; Liu, N.; Chai, W.; Gong, Q.; Wang, N.N. Heterologous expression of ATG8c from soybean confers tolerance to nitrogen deficiency and increases yield in arabidopsis. *PLoS ONE* **2012**, *7*, e37217. [[CrossRef](#)] [[PubMed](#)]
56. Chen, C.J.; Chen, H.; He, Y.H.; Xia, R. TBtools, a Toolkit for biologists integrating various biological data handling tools with a user-friendly interface. *bioRxiv* **2018**. [[CrossRef](#)]
57. Wan, Q.; Xu, R.; Li, X. Proton release by tea plant (*Camellia sinensis* L.) roots as affected by nutrient solution concentration and pH. *Plant Soil Environ.* **2012**, *58*, 429–434. [[CrossRef](#)]
58. Livak, K.J.; Schmittgen, T.D. Analysis of relative gene expression data using real-time quantitative PCR and the $2^{-\Delta\Delta C_T}$ method. *Methods* **2001**, *25*, 402–408. [[CrossRef](#)]
59. Zhang, C.; Zhang, W.; Ren, G.; Li, D.; Cahoon, R.E.; Chen, M.; Zhou, Y.; Yu, B.; Cahoon, E.B. Chlorophyll synthase under epigenetic surveillance is critical for vitamin E synthesis, and altered expression affects tocopherol levels in arabidopsis. *Plant Physiol.* **2015**, *168*, 1503–1511. [[CrossRef](#)]
60. Clough, S.J.; Bent, A.F. Floral dip: A simplified method for *Agrobacterium*-mediated transformation of *Arabidopsis thaliana*. *Plant J.* **1998**, *16*, 735–743. [[CrossRef](#)]
61. Rosen, H. A modified ninhydrin colorimetric analysis for amino acids. *Arch. Biochem. Biophys.* **1957**, *67*, 10–15. [[CrossRef](#)]



© 2020 by the authors. Licensee MDPI, Basel, Switzerland. This article is an open access article distributed under the terms and conditions of the Creative Commons Attribution (CC BY) license (<http://creativecommons.org/licenses/by/4.0/>).